Bioresource Technology 152 (2014) 267–274

Contents lists available at ScienceDirect

Bioresource Technology

journal homepage: www.elsevier.com/locate/biortech

Thermogravimetric investigation on the degradation properties and combustion performance of bio-oils

Xueyong Ren [a,b], Jiajia Meng [a], Andrew M. Moore [a], Jianmin Chang [b], Jinsheng Gou [b], Sunkyu Park [a,*]

[a] Department of Forest Biomaterials, North Carolina State University, Raleigh, NC 27695, USA
[b] College of Materials Science and Technology, Beijing Forestry University, Beijing 100083, PR China

HIGHLIGHTS

- The degradation and combustion properties of bio-oils were quantitatively evaluated.
- The formation and effect of carbonaceous solid during bio-oil combustion were studied.
- A higher amount of carbonaceous solid was produced from aged bio-oil.
- Bio-oil from torrefied wood has comparable thermal profiles with raw bio-oil.
- Bio-oils have comparable combustion index with fuel oils used in boilers.

ARTICLE INFO

Article history:
Received 19 September 2013
Received in revised form 7 November 2013
Accepted 11 November 2013
Available online 19 November 2013

Keywords:
Bio-oil
Degradation
Combustion performance
Fuel oils
Thermogravimetric analysis

ABSTRACT

The degradation properties and combustion performance of raw bio-oil, aged bio-oil, and bio-oil from torrefied wood were investigated through thermogravimetric analysis. A three-stage process was observed for the degradation of bio-oils, including devolatilization of the aqueous fraction and light compounds, transition of the heavy faction to solid, and combustion of carbonaceous residues. Pyrolysis kinetics parameters were calculated via the reaction order model and 3D-diffusion model, and combustion indexes were used to qualitatively evaluate the thermal profiles of tested bio-oils for comparison with commercial oils such as fuel oils. It was found that aged bio-oil was more thermally instable and produced more combustion-detrimental carbonaceous solid. Raw bio-oil and bio-oil from torrefied wood had comparable combustion performance to fuel oils. It was considered that bio-oil has a potential to be mixed with or totally replace the fuel oils in boilers.

© 2013 Elsevier Ltd. All rights reserved.

1. Introduction

Due to the shortages of and environmental issues associated with petroleum oil, bio-crude liquid from fast pyrolysis of renewable biomass has received a lot of attention (Bridgwater, 2012; Ma et al., 2012; Mohan et al., 2006). Like other biomass fuels, pyrolysis bio-oil can be considered essentially carbon neutral and has very low sulfur content compared to fossil fuels. Bio-oil can be a substitute for fuel oil or diesel in many static applications including boilers, furnaces, engines, and turbines for electricity generation (Czernik and Bridgwater, 2004). The combustion of bio-oil was compared with No. 2 and No. 4 fuel oils in a pilot-stabilized swirl burner and it was found that No. 4 fuel oil is more comparable to bio-oil because of its non-distillable fraction, fuel nitrogen, and ash content (Tzanetakis et al., 2011). Some efforts were reported for producing hydrogen from bio-oil by catalytic steam reforming (Xu et al., 2010) or thermal plasma technologies (Guénadou et al., 2011). Recently, bio-oil was also tested as a raw material for gasification to produce syngas (Chhiti et al., 2011).

The most important difference between bio-oil and petroleum oil is the high oxygen content of bio-oil (∼up to 55%) (Mohan et al., 2006). It is well known that the existence of a high amount of oxygen affects the pyrolysis and combustion properties in the utilization process of bio-oil, but it also plays an unfavorable role to deteriorate the properties over the time. This ageing happens inevitably to different degrees based on storage conditions, causing increased viscosity, decreased fluidity, and higher risk for phase separation (Diebold, 2002). A relatively simple process, torrefaction as a mild thermal pretreatment, was suggested to improve the thermochemical quality of biomass and stability of bio-oil by reducing the oxygen content of bio-oil (Meng et al., 2012; Srinivasan et al., 2012; Zheng et al., 2012). The reduction of oxygen in bio-oil was achieved by the decrease in hemicellulose fraction and water during the integration of torrefaction and the pyrolysis process (Zheng, 2012).

---

* Corresponding author. Tel.: +1 919 515 0473; fax: +1 919 515 6302.
E-mail address: sunkyu_park@ncsu.edu (S. Park).

0960-8524/$ - see front matter © 2013 Elsevier Ltd. All rights reserved.
http://dx.doi.org/10.1016/j.biortech.2013.11.028

The thermal-degradation property of bio-oil is of vital importance for its thermo-chemical use or upgrading process involved with heat treatment (Liu et al., 2013). However, the degradation of bio-oil occurring under pyrolysis/combustion conditions is a complex process that usually involves vaporization and thermal cracking reactions with the formation of vapors, tars, and char residues (Chhiti, 2012). Until now, the fundamental behavior and mechanisms relative to degradation (pyrolysis/combustion) of bio-oil have not been fully understood. Moreover, to the best of authors' knowledge, an in-depth comparison on the degradation behavior and combustion performance between pyrolysis bio-oil and fuel oil using thermogravimetric (TG) analyzer has not yet been reported.

In this study, a high resolution thermogravimetric analyzer was used to investigate the thermal decomposition process of different types of bio-oils. TG analysis is a widely used technique to study thermal decomposition properties and reaction mechanisms of samples undergoing a thermo-chemical reaction process (Ambalae et al., 2006; Li et al., 2011; Syed et al., 2011). The pyrolysis kinetics and combustion index analysis were performed to evaluate the thermal behavior and combustion performance of bio-oils compared to that of commercial petroleum oils.

2. Methods

2.1. Materials

Bio-oil was produced with a lab-scale fluidized bed pyrolysis reactor at 500 °C from Loblolly Pine wood without bark. Pyrolysis bio-oils were produced from untreated and torrefied wood material and the torrefaction was conducted with the absence of oxygen at 300 °C for 3 min. Aged bio-oil was obtained from the ageing treatment of bio-oil in oven at 80 °C for 24 h. The detailed information regarding the fast pyrolysis process of woody biomass for producing bio-oil can be found in the previous report (Meng et al., 2012). Physical properties and chemical composition of bio-oil used in this study are summarized in Tables 1 and S1 (Supplementary materials).

Commercial gasoline (octane 93) and diesel were purchased from a local gas station. A typical gasoline consists of hydrocarbons with between 4 and 12 carbon atoms per molecule (Dabelstein, 2007) and up to 10% ethanol. A typical diesel is composed of about 75% saturated hydrocarbons (primarily paraffins), and 25% aromatic hydrocarbons (including naphthalenes and alkylbenzenes) (Agency for Toxic Substances & Disease Registry, 1995), commonly as a mixture of carbon chains with between 8 and 21 carbon atoms per molecule (Collins, 2007). Commercial motor oil (SAE 10W-30, Old World Industries, LLC) was purchased, which consist mainly of hydrocarbons, polyalphaolefins, and polyinternal olefins, together with a minor amount of esters and additives such as detergents and dispersants. Commercial No. 2 and No. 6 fuel oil, originally used as heating sources for the boiler, were kindly provided by a local paper mill.

2.2. Thermogravimetric analysis

The thermal analysis was performed with a thermogravimetric analyzer (Q500, TA instruments). For each TG experiment, three droplets of bio-oil sample (~50 mg) were put into a platinum pan via a glass pipet. TG curves were obtained at a heating rate of 20 °C/min in this study between ambient temperature and 700 or 850 °C. Pyrolysis of bio-oil was also performed at two additional heating rates (10 and 30 °C/min) for comparison. Industrial grade nitrogen and air were used as the purge gas at a flow rate of 100 mL/min both for pyrolysis and combustion conditions. Data was analyzed using TA Instruments Universal Analysis 2000 software.

2.3. Elemental analysis and heating value

Carbon, hydrogen, and nitrogen analyses of the carbonaceous residue after the TGA experiment were performed in triplicate according to ASTM-D2591 using a Perkin Elmer CHN elemental analyzer. Oxygen content was calculated by difference. The high heating value (HHV) of bio-oils and carbonaceous residue was calculated based on elemental composition data according to Demirbas's method (Demirbas, 1997).

2.4. Pyrolysis kinetics analysis method

The pyrolysis kinetic parameters were obtained as follows. Generally, the reaction rate is expressed by the disappearance of the sample, so the degradation rate of the material can be modeled using Eq. (1).

$$\frac{d\alpha}{dt} = k\,f(\alpha) \tag{1}$$

where $f(\alpha)$ is the relationship formula of degradation and rate constant, α is the fraction of materials degraded at time t, and k is the rate constant that obeys the Arrhenius correlation, given by the following Eq. (2).

$$K = A\,\exp\,(-E/RT) \tag{2}$$

where A is the frequency factor, E is the activation energy of the reaction, R is the universal gas constant, 8.314 J/(mol K), and T is the reaction temperature.

For a linear heating rate of β

$$dT = \beta\,dt \tag{3}$$

Combining Eqs. (1)–(3) with integration, Eq. (4) is obtained for $g(\alpha)$

$$\int_0^1 \frac{d\alpha}{f(\alpha)} = \frac{A}{\beta}\int_0^T e^{-E/RT}\,dT = g(\alpha) \tag{4}$$

By following Coats and Redfern methods (Coats and Redfern, 1964), the integral form of Eq. (5) is

$$\ln\left[\frac{g(\alpha)}{T^2}\right] = \ln\left[\frac{AR}{\beta E}\left(1-\frac{2RT}{E}\right)\right] - \frac{E}{RT} \tag{5}$$

By plotting the mass loss data from the TG curves, kinetics parameters are obtained and the appropriateness for the form of $g(\alpha)$ can also be evaluated (Liu et al., 2013; Guo and Lua, 2001).

Generally, a plot of $\ln\left[\frac{g(\alpha)}{T^2}\right]$ versus $1/T$ is a straight regressive line with a slope of E/R. After determining the value of E, the arithmetic mean value of $(1-\frac{2RT}{E})$ can be calculated with initial and final reaction temperatures. Then, the frequency factor (A) can be obtained from the intercept of the line.

The expression of $g(\alpha)$ giving the comparatively high regression coefficient is considered to be representative of the sample's pyrolysis reaction order and mechanism, which can be acquired by several tentative plotting with different forms.

In this paper, the reaction order model ($n = 3$) and 3D-diffusion model (Guo and Lua, 2001) were used to obtain the kinetics parameters (Eqs. (6 and 7)), which actually show high regression adjustability, especially the reaction order model ($R^2 > 0.99$).

$g(\alpha)$ given by the reaction order model ($n = 3$),

$$g(\alpha) = \frac{[(1-\alpha)^{-2} - 1]}{2} \tag{6}$$

Table 1
Physical properties and elemental composition of bio-oils and carbonaceous residue.

Sample ID	Physical properties			Elemental composition					HHV[b] (MJ/kg)
	Viscosity (cSt)	Water (wt%)	TAN (mg KOH/g)	C (wt%)	H (wt%)	N (wt%)	O[a] (wt%)	C/O	
Raw bio-oil	11.0	21.8	85.5	39.2	7.6	0.41	52.8	0.74	15.8
Aged bio-oil	23.5	24.0	96.2	38.8	7.5	0.48	53.3	0.73	15.4
Bio-oil from torrefied wood	17.4	20.6	80.2	44.1	7.3	0.37	48.3	0.91	17.7
Carbonaceous residue from raw bio-oil pyrolysis	N.D.	N.D.	N.D.	89.0	2.5	0.38	8.2	10.9	32.1

[a] Oxygen content was calculated by difference.
[b] HHV: high heating value, calculated by HHV = (33.5[C] + 142.3[H] − 15.4[O] − 14.5[N]) × 10^{-2}.

$g(\alpha)$ given by the 3D-diffusion model,

$$g(\alpha) = \left[1 - (1-\alpha)^{1/3}\right]^2 \tag{7}$$

2.5. Combustion characteristics analysis method

In order to evaluate the combustion properties of bio-oil, several parameters used for coal and tobacco combustion (Li et al., 2011; Niu et al., 2011) were defined in this study. Due to the high resolution TGA used here, several splitting peaks were formed and made DTG curves inconsecutive. In order to get the continuous DTG curves for identifying and analyzing the combustion parameters, each original DTG curve was carefully smoothed at a smoothing region width of 2 °C by TA Instruments Universal Analysis Software.

T_i, the ignition temperature, is constructed as follows. A line is drawn across the peak of the DTG curve and produces an intersection with the TG curve. Then, a tangent line of the TG curve is drawn through this intersection point. In addition, another tangent line is drawn based on the initial part of the TG curve. Then, two tangent lines intersect at a spot and the corresponding temperature of this spot is the ignition temperature, as shown in Fig. 1.

$\mathrm{DTG_{max}}$, the peak of the DTG curve, is the maximum value of the mass-loss rate during the combustion process.

$T_{\max}$ is the corresponding temperature of the $\mathrm{DTG_{max}}$.

T_b, the burn out temperature, is defined as the temperature at which conversion (α) of 98% is achieved during one combustion stage or the entire process.

Particularly, bio-oil has two combustion regions in DTG curves, which need to be investigated separately. Therefore, T_m is defined as the temperature corresponding to the lowest point in DTG curves between two peaks and divides two stages.

The conversion is defined on the basis of the combustible part of the material and is described as,

$$\alpha_T = \frac{w_0 - w_T}{w_0 - w_f} \times 100\% \tag{8}$$

where w_T is the mass at temperature T and w_0 and w_f are the masses at the beginning and end of the combustion.

The ignition index, D_i, and the burnout index, D_b, are determined using Eqs. (9 and 10), respectively.

$$D_i = \frac{\mathrm{DTG_{max}}}{T_{\max} \times T_i} \tag{9}$$

$$D_b = \frac{\mathrm{DTG_{max}}}{\Delta T_{0.5} \times T_{\max} \times T_i} \tag{10}$$

where $\Delta T_{0.5}$ is the half peak width of the DTG curves, namely the temperature difference between the two temperatures at the mass loss rate of $\mathrm{DTG_{max}}$ by a factor of 0.5.

Further, one integration combustion index parameter, S, is defined as

$$S = \frac{\mathrm{DTG_{max}} \times \mathrm{DTG_{mean}}}{T_i^2 \times T_b} \tag{11}$$

where

$$\mathrm{DTG_{mean}} = \frac{\alpha_{T_b} - \alpha_{T_i}}{((T_b - T_i)/\beta)} \tag{12}$$

which is the average conversion rate from T_i to T_b, and β is the heating rate.

S is the integration parameter of ignition and burnout characteristic for combustion, and a higher value represents better combustion properties.

In order to compare the combustion characteristic of bio-oil with commercial oils, which feature a one-stage combustion process, a total combustion characteristics index for bio-oil was defined as the weighted mean value of the two combusting stages by the corresponding bio-oil weight-loss percentage.

3. Results and discussions

3.1. General physical properties and chemistry of bio-oils

Raw bio-oil was acidic and partly aqueous, with a TAN of 85.5 mg KOH/g and a water content of 21.8%. After accelerated ageing by heat-treatment, aged bio-oil became more acidic and had a higher viscosity and higher water content (Table 1). The solvent fractionation was conducted using water fractionation followed by diethyl ether and dichloromethane extraction according to Oasmaa's method (Oasmaa et al., 2003). It was found that, during the ageing process, the water soluble fraction partially turned water insoluble, which made the water insoluble fraction of aged bio-oil almost two times higher than that of raw bio-oil (Table S1 in Supplementary materials). Especially, the content and average molecular weight of pyrolytic lignin (heavy compounds in bio-oil) increased significantly after ageing (Kim et al., 2012). Since the elemental composition was nearly same as raw bio-oil, the heating value of aged bio-oil was quite similar to raw bio-oil. On the other hand, bio-oil from torrefied wood is distinctively different with lower water content, higher viscosity, and higher heating value, compared to raw bio-oil (Table 1).

3.2. Degradation profile for the devolatilization and combustion of raw bio-oil

Based on the TG and DTG curves, three stages (S-I, 25–330 °C; S-II: 330–490 °C; S-III, 490–700 °C) were observed and developed for the degradation of raw bio-oil with a heating rate of 20 °C/min (Fig. 1). S-I is the first stage, mainly standing for the devolatilization process with about 75% of the weight-loss of bio-oil. Water

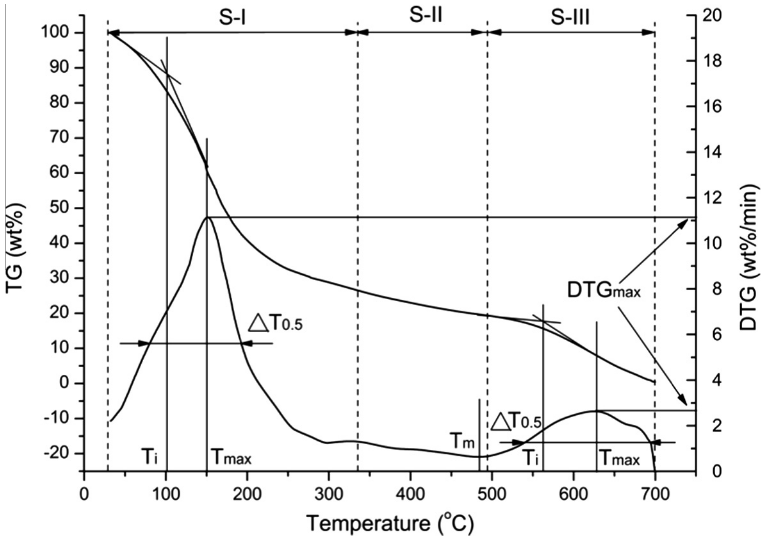

Fig. 1. Three stages of bio-oil combustion from the TG–DTG curves using raw bio-oil in an oxidative environment.

and light compounds (e.g., ketones, acids, methanol, and aldehydes) in bio-oil were volatilized (also partly oxidized under air condition) during the first stage under 330 °C, which were from mainly carbohydrates of biomass (Ba et al., 2004). S-II is a transition from the devolatilization stage to the combustion stage and the small amount of weight loss occurs in this region. Lastly, S-III is the last stage for combustion, which corresponded to about 20% of the weight-loss. It is noted that this stage only exists when oxygen is introduced.

The degradation process of bio-oil in air and nitrogen both had the S-I and S-II stages, and they were quite similar to each other with similar weight-loss rates. However, S-III was unique in the thermal decomposition of bio-oil in the presence of oxygen. Moreover, based on the comparison between pyrolysis and combustion conditions, it can be concluded that oxygen mainly acted on stage III and had little impact on stages I and II. For the devolatilization and transition stages under 490 °C, oxygen may enhance the reaction occurred at slightly lower temperatures, but may not change the volatilization pattern compared to inert condition, as shown in Figs. 2 (oxidative) and S1 (inert). For the combustion stage above 490 °C, oxygen became the key factor for the cracking of the residue material.

Figs. 2 and S1 also show the effect of the heating rate on the TG and DTG curves of bio-oil degradation in nitrogen and air. With proceeding from a heating rate of 10–30 °C/min, the degradation stage-I and II shifted to a higher temperature range with a larger weight-loss rate, but within a similar temperature range. However, as to the combustion stage III, the degradation temperature range tended to be wider and ended at higher temperatures when increasing the heating rate. Therefore, heating rate plays a different role in devolatilization and combustion stages of bio-oil. Increment of heating rate can accelerate the devolatilization rate, but combustion in stage III requires more time to complete the oxidation reaction due to the significant thermal delay.

3.3. Formation of carbonaceous solid and its role on the combustion process

After the pyrolysis experiment of bio-oil by TGA at inert environment, a porous black material was generated as a residue in the TGA platinum pan, which was identified as a carbonaceous material with a high carbon content of 89.0% and low oxygen content of 8.2% (Table 1). This carbonaceous residue was considered a product from stage-II for both pyrolysis and combustion conditions, also as the starting material for stage-III of combustion. This observation is consistent with the previous studies at a heating rate of 10 °C/min (Ba et al., 2004; Zhang et al., 2009). By using vacuum pyrolysis oil from softwood bark with a water content of 13 wt%, Ba and co-workers found that the combustion of carbonaceous solid from bio-oil mainly happened at 480 °C with a clear and higher DTG peak than the first degradation stage. Nevertheless, Zhang and co-workers only observed a very slight peak for the burning of the remainder from straw bio-oil between 420 and 480 °C. The difference of the burning intensity of secondary stage in two studies can be contributed to the different properties and components of bio-oil, which greatly affected the forming of residues during the combustion process.

The carbonaceous residue has been categorized into two kinds of solids, “fragile and thin-walled cenosphere” and “dense and glassy sphere”, which were reported from the burning process of single droplet of pine and oak oils (Wornat et al., 1994). The transformation of the glassy sphere to the enlarged cenosphere during the combustion process was also observed, which indicated that the glassy sphere was a precursor to the cenosphere.

It is worth noting to accentuate and describe the formation of cenosphere material and its effect on the combustion process of bio-oil. In the earlier stage of thermal treatment, liquid-phase polymerization of bio-oil happened due to its nature of high surface tension and increasing viscosity. However, oxygenate-rich vapors under the effect of heat tended to escape from the droplet with disrupting the rigid core, resulting in a micro-explosion inside of the bio-oil with increasing ambient temperature and heat absorption (Ba et al., 2004; Wornat et al., 1994). Micro-explosions phenomena, especially explosion times and frequency of bio-oil droplets, were also observed and reported in detail by high-speed photography (Teixeira et al., 2013). The size of the droplet grew gradually while keeping its spherical form under the vapor pressure effect. As a result of these several synthetic reactions, a carbonaceous and macro-porous solid material was formed.

Generally, two kinds of reactions with reverse resulting directions happen competitively in the later stages of bio-oil degradation, which are cracking for decomposition and charring for polymerization. Initially, at low temperatures, charring by polymerization reactions are dominant and carbonaceous residue grows up. When the temperature is properly higher with enough oxygen, cracking reactions become dominant and the charry mate-

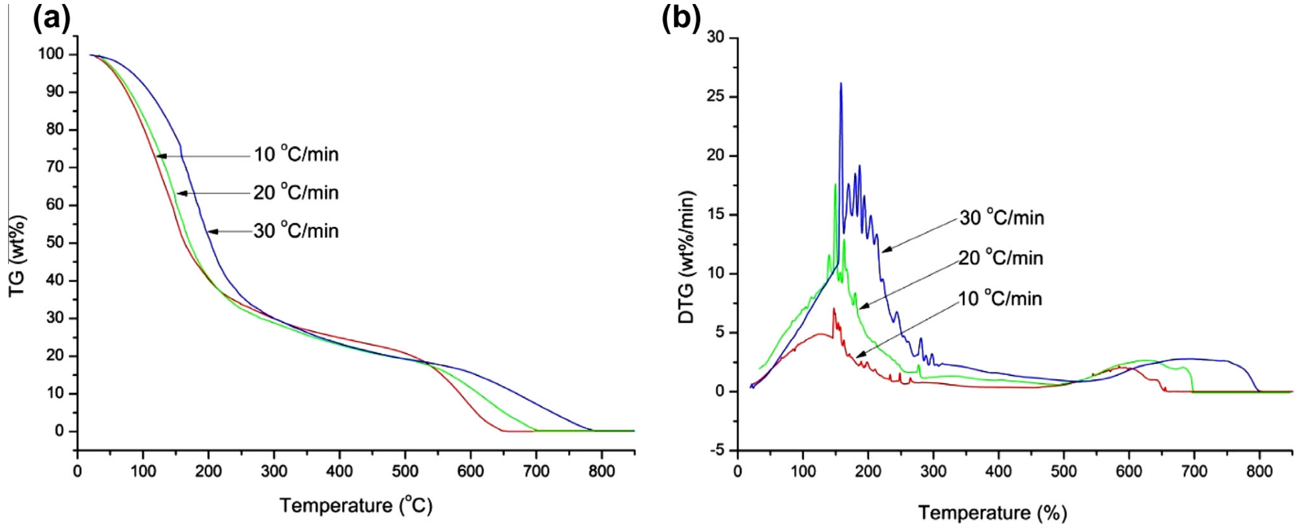

Fig. 2. Degradation of raw bio-oil at different heating rates in oxidative environment: (a) TG curves and (b) DTG curves.

rial begins to collapse. From the viewpoint of thermal conversion efficiency, the cenosphere structure is unfavorable for the heat and mass transfer inside the carbonaceous matrix, and plays an inhibiting role in the thoroughly degradation of bio-oil, which might be the reason for the existence of stage-II with a long "dead time" and low degradation rate. This could explain why bio-oil is hard to fully ignite. In general, ideal combustion of bio-oil prefers little formation of carbonaceous solid, as they are hard to decompose and require high temperatures.

3.4. Pyrolysis properties and kinetics parameters of bio-oils

The overall pattern for pyrolysis profiles of raw bio-oil, aged bio-oil, and bio-oil from torrefied wood were similar in terms of DTG peak, but they were degraded at different temperatures (Fig. 3). Aged bio-oil began to degrade at higher temperatures and produced more residues, which was due to its much higher water insoluble fraction compared to that of raw bio-oil (Table S1). Bio-oil from torrefied wood had a similar weight-loss rate under 200 °C with aged bio-oil, but showed a higher weight-loss rate between 200 and 400 °C and had a similar char yield as raw bio-oil. This phenomenon can be attributed to the higher amount of high molecular mass and lower content of low molecular mass fraction in bio-oil from torrefied biomass compared to that of raw bio-oil (Meng et al., 2012).

Kinetic parameters for the pyrolysis reaction of bio-oil were obtained in Table 2 by the reaction order model and 3-D diffusion model, which are controlled by the inherent order of reactions and the mass/heat transfer, respectively. These two models showed the similar trend of kinetic parameters and confirmed with each other for these bio-oil samples. However, it is still an open question which model accurately describes the pyrolysis process with respect to the reaction mechanisms, since the nature of biomass pyrolysis is very sophisticated. Although the regression coefficients are higher for reaction order model, 3D diffusion model also show a close correlation. Considering the high coefficients in two models (all over 0.9) and the small difference between them, it appears that both models can explain biomass pyrolysis behavior. Apparent activation energy obtained by the reaction order model ranges within 30–38 kJ/mol for bio-oils tested, while the value obtained by the 3-D diffusion model ranges from 36 to 48 kJ/mol. The frequency factors showed here are in the order of 10^3–10^4 min^{-1}. These values are comparable to the data on the bio-oil from corn, rice husk, and swine manure (Xiu et al., 2012; Zhang et al., 2009). As the heating rate increased from 10 to 30 °C/min, the activation energy and frequency factor

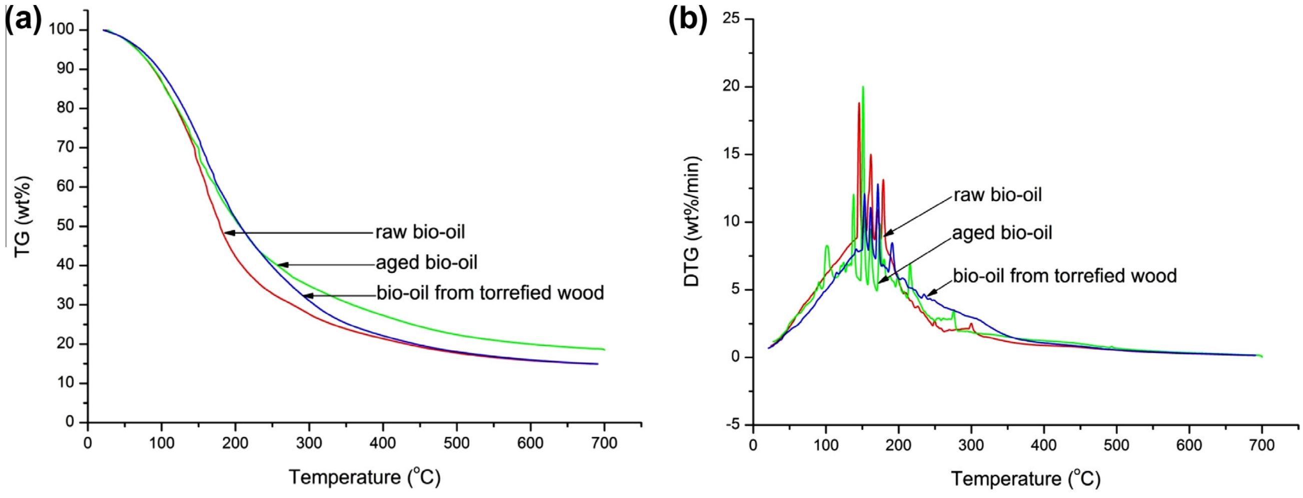

Fig. 3. Degradation of raw bio-oil, aged bio-oil, and bio-oil from torrefied wood in inert environment: (a) TG curves and (b) DTG curves.

Table 2
Pyrolysis kinetic parameters of bio-oils.

Samples	Heating rate (°C min^{-1})	Temperature range (°C)	Reaction order model			3D-diffusion model		
			E (kJ mol^{-1})	A (min^{-1})	Correlation coefficients (R^2)	E (kJ mol^{-1})	A (Min^{-1})	Correlation coefficients (R^2)
Raw bio-oil	10	28–440	31.1	2.42×10^3	0.993	40.6	1.41×10^3	0.918
	20	30–478	34.7	10.4×10^3	0.997	41.6	1.43×10^3	0.927
	30	33–491	37.7	23.6×10^3	0.996	47.5	6.02×10^3	0.952
Aged bio-oil	20	31–483	30.2	2.03×10^3	0.994	36.5	0.22×10^3	0.910
Bio-oil from torrefied wood	20	32–492	34.4	6.74×10^3	0.991	41.2	0.92×10^3	0.964

both increased due to the higher degradation intensity by larger thermal flux.

According to the chemical kinetics, activation energy is defined as the energy barrier that must be exceeded in order for a chemical reaction to occur and frequency factor is a reflection of the frequency of collisions between reacting molecules, which describe the number of potential elementary reactions per unit time. Aged bio-oil has a lower apparent activation energy than bio-oil from raw biomass, which indicates that aged bio-oil is easier to degrade and is more thermally instable. Reduction of frequency factor for aged bio-oil can be explained by the lesser accessibility of oil components due to its increasing molecular dimension caused by polymerization in the ageing process. Bio-oil from torrefied wood had a similar apparent activation to that of raw bio-oil, but a lower frequency factor. Torrefaction was thought mainly to change the bio-oil composition in terms of quantities of same oil species rather than producing significant amount of different compounds (Meng et al., 2012). However, bio-oil from torrefied wood was more concentrated in lignin-derived compounds but with less acids, aldehydes, ketones, etc., which turned out to be less chemically active, resulting in a slightly lower frequency factor.

3.5. Combustion performance and index analysis of bio-oils

Along with the pyrolysis/thermal degradation process of bio-oil in inert condition, combustion performance of bio-oil was also studied by TGA in oxidation environment, which is vital for evaluating its potential as heating fuel. Comparing to raw bio-oil, aged bio-oil and bio-oil from torrefied wood had similar devolatilization and combustion profiles with three stages for the entire time in terms of DTG profiles (Fig. 4). During stage-I, DTG peaks of aged bio-oil and bio-oil from torrefied wood shifted to higher temperatures with lower weight-loss intensities. There was no clear difference between these bio-oil samples in transition stage-II. In the end of stage II at ~490 °C, different mass percentages of carbonaceous solid were produced, and aged bio-oil had the largest carbonaceous solid content compared to the other two bio-oils. In stage-III, the DTG peaks were located in the same temperature range but had different intensities, with aged bio-oil as the highest, followed by bio-oil from torrefied wood in the middle, and raw bio-oil as the lowest one.

Tables 3 shows the calculated combustion index of bio-oils in both devolatilization and combustion stages. Corresponding combustion parameters are shown in Table S2. The calculated combustion characteristic index for the two degradation stages of bio-oil were within different number ranges, and the index of the former were all two orders of magnitude larger than the latter. This is simply due to the higher degradation temperature of the combustion stage. Comprehensively speaking, ideal combustion prefers less mass degrading in the later stage because of the much lower combustion index. With increasing heating rate, the combustion index of the earlier stage for raw bio-oil was promoted, but that of the later stage varied less. Therefore, it is clear that the heating rate had a clear effect on the combustion index of raw bio-oil in the devolatilization stage, but was less effective on the combustion stage.

In the devolatilization stage, bio-oil from torrefied wood had a slightly lower but still comparable index as raw bio-oil, while aged bio-oil had a much lower one. During the combustion stage, aged bio-oil and bio-oil from torrefied wood all had better combustion indexes compared to that of raw bio-oil in terms of ignition, burnout, and integration performance. However, it needs to be

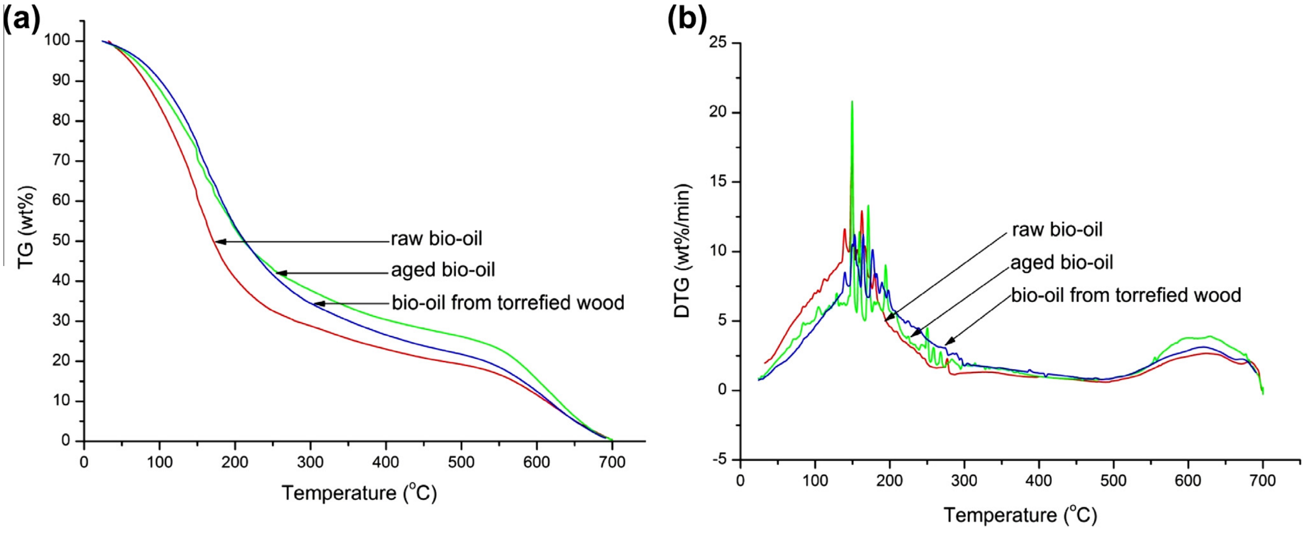

Fig. 4. Degradation of raw bio-oil, aged bio-oil, and bio-oil from torrefied wood in oxidative environment: (a) TG curves and (b) DTG curves.

Table 3
Combustion characteristic indices of bio-oils during the devolatilization stage and combustion stage; ignition index (D_i) burnout index (D_b), and combustion index (S).

Samples	Heating rate (°C min^{-1})	Devolatilization stage (Stage I and II)			Combustion stage (Stage III)		
		$D_i \times 10^{-4}$ (wt% in^{-1} °C^{-2})	$D_b \times 10^{-6}$ (wt% min^{-1} °C^{-3})	$S \times 10^{-6}$ (wt%^{2} min^{-2} °C^{-3})	$D_i \times 10^{-6}$ (wt% min^{-1} °C^{-2})	$D_b \times 10^{-8}$ (wt% min^{-1} °C^{-3})	$S \times 10^{-8}$ (wt%^{2} min^{-2}°C^{-3})
Raw bio-oil	10	4.28	3.45	4.69	6.30	6.08	1.88
	20	9.24	10.75	11.61	7.63	5.04	2.86
	30	7.01	6.46	11.66	6.56	3.19	2.51
Bio-oil from torrefied wood	20	6.82	6.91	8.49	9.12	6.15	3.94
Aged bio-oil	20	3.10	1.74	2.37	11.0	8.27	5.80

Table 4
Total combustion characteristics of bio-oil compared with gasoline, diesel, and motor oil at 20 °C min^{-1}.

Samples	Total combustion characteristics index		
	$D_i \times 10^{-4}$ (wt% min^{-1} °C^{-2})	$D_b \times 10^{-6}$ (wt% min^{-1} °C^{-3})	$S \times 10^{-6}$ (wt%^{2} min^{-2} °C^{-3})
Raw bio-oil	7.45	8.66	9.35
Bio-oil from torrefied wood	5.31	5.37	6.60
Aged bio-oil	2.27	1.28	1.73
Motor oil	2.88	5.38	9.56
Diesel	5.68	4.98	51.3
Gasoline	61.9	73.1	1820
No. 2 fuel oil	6.68	6.06	64.47
No. 6 fuel oil	1.09	0.28	3.11

emphasized that aged bio-oil had a larger percentage of mass degraded in the later stage-III with harsher conditions and a much lower corresponding combustion index. Therefore, based on the total combustion index with integration of the whole degradation process (Table 4), aged bio-oil had a much lower combustion index, with only one fifth of that of raw bio-oil. Nevertheless, bio-oil from torrefied wood had a comparable combustion performance as raw bio-oil. These results can not only be attributed to the compositional difference, but also originated from the different tendency for the forming of carbonaceous solid during the combustion process. Aged bio-oil produced more solid material that can only be combusted at high temperatures, which are detrimental for combustion performance.

3.6. Combustion performance of bio-oil compared with commercial oils

Fig. 5 shows the combustion process of bio-oil compared with gasoline, diesel, motor oil, and fuel oils by TGA. It can be found that the combustion of commercial fuel oils was with one entire process, which makes a clean burning, rather than burning in two stages as bio-oil burns. Compared with the early combustion stage of bio-oil, gasoline volatilized at a lower temperature, and diesel showed a similar combustion temperature range, while motor oil degraded at a higher temperature. No. 2 fuel oil has an identical thermal profile with that of diesel, while No. 6 fuel oil has a much broader decomposition range from 150 °C to nearly 600 °C. In regards to the combustion index in Table 4, the performance of bio-oil is comparable to fuel oils. More specifically, the ignition and burnout index of raw bio-oil are close to those of the No. 2 fuel oil, while its integration combustion index is more similar to No. 6 fuel oil. The somewhat similar degradation profile of bio-oil and fuel oils may be one of the practical reasons for the possibility of emulsifying upgraded or partly crude bio-oil into boilers and low-quality diesel engine. Replacing heavy fuel oil (HFO) in industrial or district boilers is regarded as the near-term future use for bio-oil (Oasmaa et al., 2010), as HFO boilers are typically larger and more robust than the fired boilers of light fuel oil (LFO).

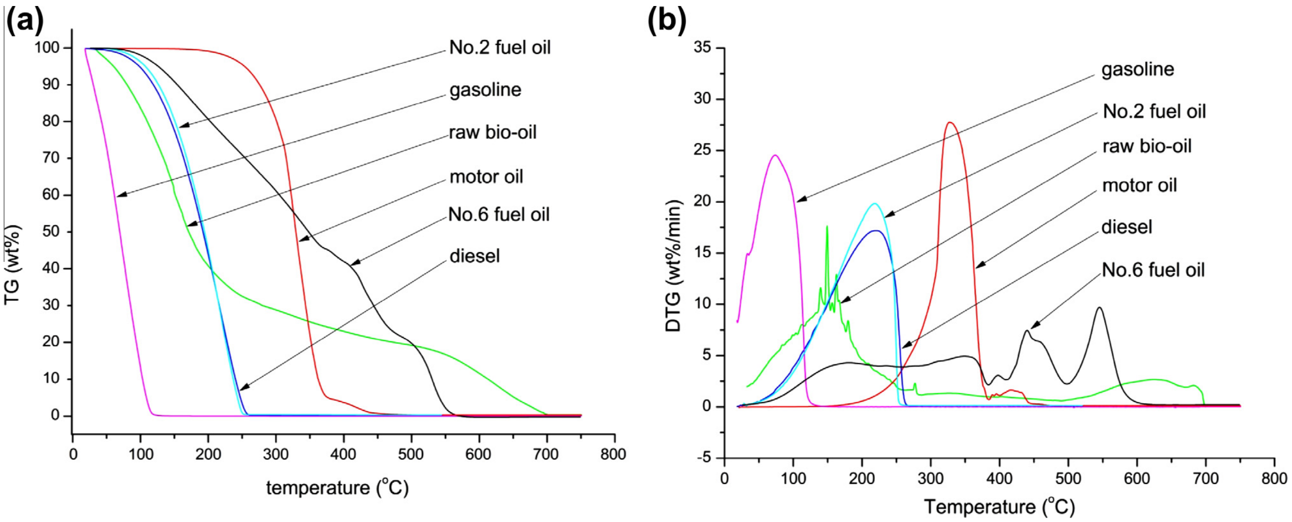

Fig. 5. Degradation of raw bio-oil, gasoline, diesel, motor oil, and No. 2 and No. 6 fuel oil in oxidative environment: (a) TG curves and (b) DTG curves.

However, bio-oil had better ignition properties than several common petroleum oils, such as diesel, motor oil, and fuel oils which may explain the high oxygen content in bio-oil. Based on these observations, bio-oil has a potential to be mixed with conventional fuel oils, but further studies need to be performed.

4. Conclusion

Degradation process and combustion behavior of raw bio-oil, aged bio-oil, and bio-oil from torrefied wood were extensively studied and compared. Based on the thermogravimetric analysis, a three-stage degradation process was identified. It was found that carbonaceous solid was formed gradually during the degradation of bio-oil, which contributes to its incomplete burning at the initial stage and much lower combustion index compared to commercial gasoline, diesel, or light fuel oil. Aged bio-oil was more thermal instable and generated a higher amount of carbonaceous solid. Raw bio-oil and bio-oil from torrefied wood were found to have comparable combustion performance with fuel oils.

Acknowledgements

Authors acknowledge the financial support from the China Scholarship Council (CSC), File No. 201206510009 and USDA Agriculture and Food Research Initiative Competitive Grant No. 2011-68005-30410.

Appendix A. Supplementary data

Supplementary data associated with this article can be found, in the online version, at http://dx.doi.org/10.1016/j.biortech.2013.11.028.

References

Agency for Toxic Substances & Disease Registry, 1995. Toxicology profile for fuel oils. P.H.S., U.S. Department of Health and Human Services (Ed.). Atlanta, GA, pp. 105–109.

Ambalae, A., Mahinpey, N., Freitag, N., 2006. Thermogravimetric studies on pyrolysis and combustion behavior of a heavy oil and its asphaltenes. Energy Fuels 20, 560–565.

Ba, T.Y., Chaala, A., Garcia-Perez, M., Rodrigue, D., Roy, C., 2004. Colloidal properties of bio-oils obtained by vacuum pyrolysis of softwood bark. Characterization of water-soluble and water-insoluble fractions. Energy Fuels 18, 704–712.

Bridgwater, A.V., 2012. Review of fast pyrolysis of biomass and product upgrading. Biomass Bioenergy 38, 68–94.

Chhiti, Y., Salvador, S., Commandre, J.M., Broust, F., Couhert, C., 2011. Wood bio-oil noncatalytic gasification: influence of temperature, dilution by an alcohol and ash content. Energy Fuels 25, 345–351.

Chhiti, Y., Salvador, S., Commandré, J.-M., Broust, F., 2012. Thermal decomposition of bio-oil: focus on the products yields under different pyrolysis conditions. Fuel 102, 274–281.

Coats, A.W., Redfern, J.P., 1964. Kinetic parameters from thermogravimetric data. Nature 201, 68–69.

Czernik, S., Bridgwater, A.V., 2004. Overview of applications of biomass fast pyrolysis oil. Energy Fuels 18, 590–598.

Collins, C.D., 2007. Implementing phytoremediation of petroleum hydrocarbons. In: Methods in Biotechnology, vol. 23, N. Willey Humana Press Inc., pp. 99–108.

Demirbas, A., 1997. Calculation of higher heating values of biomass fuels. Fuel 76, 431–434.

Diebold, J.P., 2002. A review of the chemical and physical mechanisms of the storage stability of fast pyrolysis bio-oils. In: Bridgwater, A.V. (Ed.), Fast Pyrolysis of Biomass: A Handbook. CPL Press, Newbury, UK, pp. 243–292.

Dabelstein, W., Reglitzky, A., Schutze, A., Reders, K., 2007. Automotive fuels. Ullmann's Encyclopedia of Industrial Chemistry, vol. 4. Wiley-VCH, Weinheim, pp. 425–458.

Guénadou, D., Lorcet, H., Peybernès, J., Catoire, L., Osmont, A., Gökalp, I., 2011. Plasma thermal conversion of bio-oil for hydrogen production. Int. J. Energy Res. 36, 409–414.

Guo, J., Lua, A.C., 2001. Kinetic study on pyrolytic process of oil-palm solid waste using two-step consecutive reaction model. Biomass Bioenergy 20, 223–233.

Kim, T.-S., Kim, J.-Y., Kim, K.-H., Lee, S., Choi, D., Choi, I.-G., Choi, J.W., 2012. The effect of storage duration on bio-oil properties. J. Anal. Appl. Pyrolysis 95, 118–125.

Li, X.G., Lv, Y., Ma, B.G., Jian, S.W., Tan, H.B., 2011. Thermogravimetric investigation on co-combustion characteristics of tobacco residue and high-ash anthracite coal. Bioresour. Technol. 102, 9783–9787.

Liu, S., Chen, M., Hu, Q., Wang, J., Kong, L., 2013. The kinetics model and pyrolysis behavior of the aqueous fraction of bio-oil. Bioresour. Technol. 129, 381–386.

Ma, L., Wang, T., Liu, Q., Zhang, X., Ma, W., Zhang, Q., 2012. A review of thermal–chemical conversion of lignocellulosic biomass in China. Biotechnol. Adv. 30, 859–873.

Meng, J., Park, J., Tilotta, D., Park, S., 2012. The effect of torrefaction on the chemistry of fast-pyrolysis bio-oil. Bioresour. Technol. 111, 439–446.

Mohan, D., Pittman, C.U., Steele, P.H., 2006. Pyrolysis of wood/biomass for bio-oil: a critical review. Energy Fuels 20, 848–889.

Niu, S.L., Han, K.H., Lu, C.M., 2011. Characteristic of coal combustion in oxygen/carbon dioxide atmosphere and nitric oxide release during this process. Energy Convers. Manage. 52, 532–537.

Oasmaa, A., Kuoppala, E., Solantausta, Y., 2003. Fast pyrolysis of forestry residue.2. Physicochemical composition of product liquid. Energy Fuels 17, 433–443.

Oasmaa, A., Solantausta, Y., Arpiainene, V., Kuoppala, E., Sipila, K., 2010. Fast pyrolysis bio-oils from wood and agricultural residues. Energy Fuels 24, 1380–1388.

Srinivasan, V., Adhikari, S., Chattanathan, S.A., Park, S., 2012. Catalytic pyrolysis of torrefied biomass for hydrocarbons production. Energy Fuels 26, 7347–7353.

Syed, S., Qudaih, R., Talab, I., Janajreh, I., 2011. Kinetics of pyrolysis and combustion of oil shale sample from thermogravimetric data. Fuel 90, 1631–1637.

Tzanetakis, T., Moloodi, S., Farra, N., Nguyen, B., McGrath, A., Thomson, M.J., 2011. Comparison of the spray combustion characteristics and emissions of a wood-derived fast pyrolysis liquid–ethanol blend with number 2 and number 4 fuel oils in a pilot-stabilized swirl burner. Energy Fuels 25, 4305–4321.

Teixeira, A., Hermann, R., Kruger, J., Suszynski, W., Schmidt, L., Schmidt, D., Dauenhauer, P., 2013. Microexplosions in the upgrading of biomass-derived pyrolysis oils and the effects of simple fuel processing. ACS Sustainable Chem. Eng. 1, 341–348.

Wornat, M.J., Porter, B.G., Yang, N.Y.C., 1994. Single droplet combustion of biomass pyrolysis oils. Energy Fuels 8, 1131–1142.

Xiu, S., Rojanala, H.K., Shahbazi, A., Fini, E.H., Wang, L., 2012. Pyrolysis and combustion characteristics of bio-oil from swine manure. J. Therm. Anal. Calorim. 107, 823–829.

Xu, Q.L., Lan, P., Zhang, B.Z., Ren, Z.Z., Yan, Y.J., 2010. Hydrogen production via catalytic steam reforming of fast pyrolysis bio-oil in a fluidized-bed reactor. Energy Fuels 24, 6456–6462.

Zhang, R., Zhong, Z., Huang, Y., 2009. Combustion characteristics and kinetics of bio-oil. Front. Chem. Eng. Chin. 3, 119–124.

Zheng, A., Zhao, Z., Chang, S., Huang, Z., He, F., Li, H., 2012. Effect of torrefaction temperature on product distribution from two-staged pyrolysis of biomass. Energy Fuels 26, 2968–2974.